Cell, Vol. 122, 275–287, July 29, 2005, Copyright ©2005 by Elsevier Inc. DOI 10.1016/j.cell.2005.05.031

Par-4 Links Dopamine Signaling and Depression

Sang Ki Park,[1] Minh Dang Nguyen,[1,3] André Fischer,[1,3] Margaret Po-Shan Luke,[1] El Bachir Affar,[1] Paul Brian Dieffenbach,[2] Huang-Chun Tseng,[1] Yang Shi,[1] and Li-Huei Tsai[1,*]
[1]Department of Pathology
Howard Hughes Medical Institute
Harvard Medical School
77 Avenue Louis Pasteur
Boston, Massachusetts 02115
[2]Harvard-MIT Division of Health Sciences and Technology
77 Massachusetts Avenue, E25–519
Cambridge, Massachusetts 02139

Summary

Prostate apoptosis response 4 (Par-4) is a leucine zipper containing protein that plays a role in apoptosis. Although Par-4 is expressed in neurons, its physiological role in the nervous system is unknown. Here we identify Par-4 as a regulatory component in dopamine signaling. Par-4 directly interacts with the dopamine D2 receptor (D2DR) via the calmodulin binding motif in the third cytoplasmic loop. Calmodulin can effectively compete with Par-4 binding in a Ca^{2+}-dependent manner, providing a route for Ca^{2+}-mediated downregulation of D2DR efficacy. To examine the importance of the Par-4/D2DR interaction in dopamine signaling in vivo, we used a mutant mouse lacking the D2DR interaction domain of Par-4, *Par-4ΔLZ*. Primary neurons from *Par-4ΔLZ* embryos exhibit an enhanced dopamine-cAMP-CREB signaling pathway, indicating an impairment in dopamine signaling in these cells. Remarkably, *Par-4ΔLZ* mice display significantly increased depression-like behaviors. Collectively, these results provide evidence that Par-4 constitutes a molecular link between impaired dopamine signaling and depression.

Introduction

Depression, characterized mainly by low mood, amotivation, anhedonia, low energy, and/or fatigue, is one of the most prevalent disorders, with an estimated lifetime prevalence of 16.2% in the U.S. adult population (Blazer et al., 1994) resulting in tremendous social costs (Greenberg et al., 1993). Although the cause of depression is obviously multifaceted, the "monoamine hypothesis," describing deficiency or imbalance of the monoamine systems as the cause, has been a central topic of research (Bunney and Davis, 1965; Coppen, 1967; Schildkraut et al., 1965). This hypothesis was generated and supported by the fact that most antidepressants share the property of acutely modifying the serotonin or noradrenaline levels at the synapse (Delay et al., 1952; Fuller, 1995; Kuhn, 1958; Leonard, 1978). However, since clinical effects of antidepressants are usually significantly delayed, it is now believed that an adaptation of downstream events, including changes in gene expression and/or modification of other neurotransmitter systems, due to chronic treatment underlies their antidepressant efficacy (Manji et al., 2001; Wong and Licinio, 2001). Moreover, a large percentage of depressive subjects are resistant to the current antidepressant therapies (Baldessarini, 1989), demanding improvement of therapeutic strategies.

Modulating the brain's reward and motivation circuits, governed primarily by dopamine, has been one of the attractive targets for treating depressive disorders (Kinney, 1985). Dopamine functions in target cells through five known subtypes of dopamine receptors (D1, D2, D3, D4, and D5) to regulate motor control, stereotypic behaviors, arousal, mood, motivation, and endocrine function (Missale et al., 1998). Dopamine D2 receptor (D2DR), the predominant D2-like dopamine receptor subtype, is coupled to the inhibitory G protein (Gi) to downregulate cAMP signaling upon activation (De Camilli et al., 1979). Impairment in the function of D2DR is implicated in various psychiatric disorders such as schizophrenia, mood disorders, and drug addiction (Nestler, 2001). Understanding the details of the modulatory events in D2DR-mediated intracellular signaling is believed to provide therapeutic targets for treating various associated disorders.

Prostate apoptosis response 4 (Par-4) is a leucine zipper containing protein that was initially identified as a proapoptotic factor induced by apoptotic stimuli (Sells et al., 1994). Par-4 interacts with PKCζ (Diaz-Meco et al., 1996) to interfere with the prosurvival activity of NFκB (Diaz-Meco et al., 1999). Par-4 also interacts with Wilms' tumor 1 (WT1) to inhibit the growth arrest induced by WT1 (Johnstone et al., 1996). In the nervous system, Par-4 induction has been linked to neuronal death in various neurodegenerative diseases (Duan et al., 1999b; Guo et al., 1998; Pedersen et al., 2000). Although Par-4 is prominently detected in synaptic compartments of the brain (Duan et al., 1999a), a physiological role for Par-4 in differentiated neurons has not been elucidated. In the present study, we identify Par-4 as a modulator for Ca^{2+}-dependent regulation of D2DR signaling. Based on behavioral abnormalities observed in mice with disrupted Par-4/D2DR interaction, we propose that Par-4 constitutes a missing link between D2DR signaling and the manifestation of depressive symptoms.

Results

Par-4 Directly Interacts with D2DR

To better understand the mechanisms of D2DR-mediated signaling we attempted to discover modulatory components for D2DR-mediated intracellular signaling by exploring D2DR-interacting proteins. We identified prostate apoptosis response 4, Par-4, as a D2DR-interacting protein in a yeast two-hybrid screen using a hu-

*Correspondence: li-huei_tsai@hms.harvard.edu
[3]These authors contributed equally to this work.

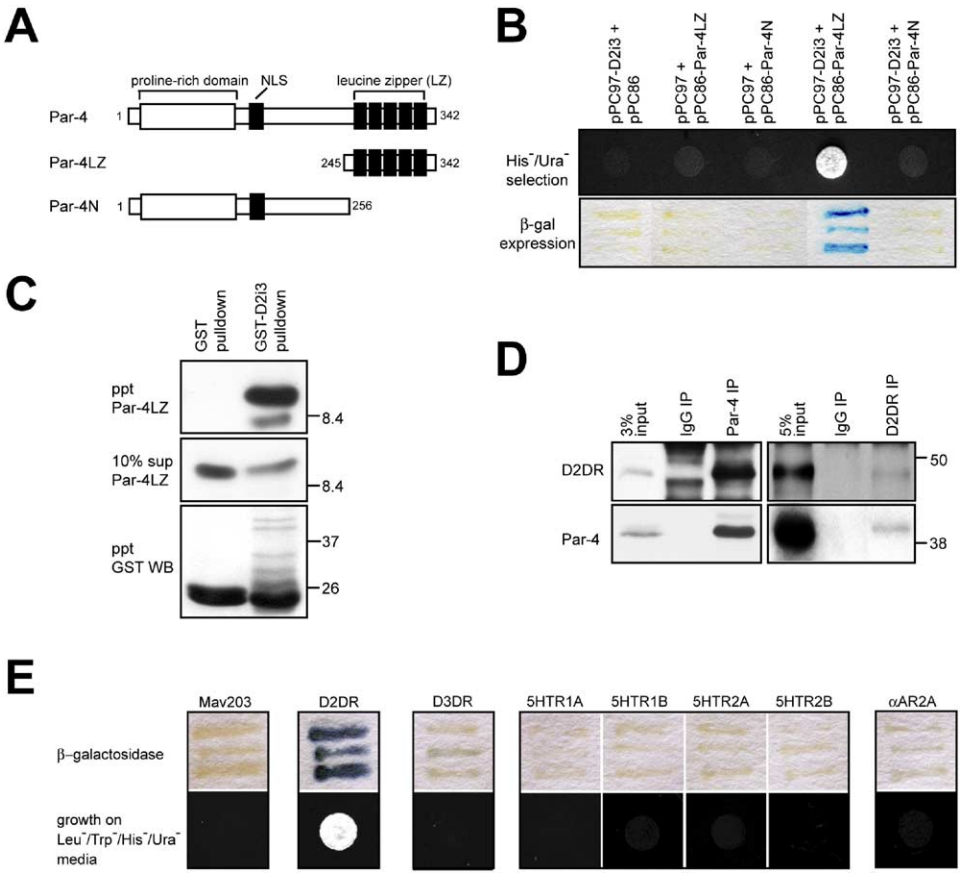

Figure 1. Interaction between Par-4 and D2DR

(A) A schematic diagram of human Par-4 protein. Par-4LZ is the protein product encoded by the cDNA clone isolated from the yeast two-hybrid screen. Numbers represent corresponding amino acid residues. NLS, nuclear localization signal.

(B) The Par-4 and D2i3 interaction in the yeast two-hybrid assay. Upper panel: growth on the Ura^-/His^-/3-AT (20 mM) media. Lower panel: β-galactosidase expression.

(C) Direct interaction between Par-4 and D2i3 in an in vitro binding assay.

(D) Coimmunoprecipitation of Par-4 and D2DR in mouse brain lysates. (Left panels) coimmunoprecipitate (CoIP) using anti-Par-4 antibody. (Right panels) CoIP with anti-D2DR antibody. Anti-rabbit anti-GST antibody and anti-rabbit anti-hemaglutinin antibody were used as negative controls for Par-4 IP and for D2DR IP, respectively.

(E) Relative specificity of Par-4 with D2DR interaction. The human cDNA coding the long third intracellular loops of various receptors were cloned into pPC97 and cotransformed Mav203 yeast cells with pPC86-Par-4LZ. The expression of interaction-dependent markers, β-galactosidase (upper panels), and growth on His^-/Ura^- media (lower panels) were examined. D2DR, dopamine D2 receptor; D3DR, dopamine D3 receptor; 5HTR, 5-hydroxytryptamine (serotonin) receptor; αAR2A, α-adrenergic receptor 2A.

man fetal embryonic brain library and the third intracellular loop of the long isoform of human D2DR (D2i3, amino acid residues 212–373) as bait. The human Par-4 cDNA clone recovered from the yeast two-hybrid screen encompasses amino acid residues 245–342 that harbor the leucine zipper domain of Par-4 (Par-4LZ, Figure 1A). The LZ domain-dependent interaction was further verified by the prominent interaction-dependent growth on His^-/Ura^- media and by β-galactosidase expression (Figure 1B). The direct interaction of Par-4 with D2i3 was demonstrated by an in vitro binding assay using purified GST-D2i3 and Par-4LZ proteins (Figure 1C). Approximately 50% of the total Par-4LZ protein was pulled down by an equimolar amount of GST-D2i3 protein. Importantly, the endogenous D2DR and Par-4 can be coimmunoprecipitated from mouse brain lysate, suggesting that the two proteins potentially form a functional complex in vivo (Figure 1D, and Figures S1 and S2 in the Supplemental Data available with this article online). Interestingly, the coimmunoprecitation revealed a predominant signal of ~48 kDa that corresponds to the proposedly monomeric, unglycosylated or mildly glycosylated D2DR species (Fishburn et al., 1995; Jarvie and Niznik, 1989). Although there is the possibility of selective enrichment in the sample preparation procedure and/or preferential detection of the D2DR species given that D2DR exists in differentially modified states in vivo, this result may suggest a functionally selective interaction of Par-4 with a subspecies of D2DR in vivo, which is yet to be investigated.

To assess the relative specificity of D2DR and Par-4 interaction, we investigated whether Par-4 interacts with other structurally and functionally related G protein-coupled receptors, including the dopamine D3 receptor. In yeast two-hybrid assays, no significant interaction-dependent marker expression was detected

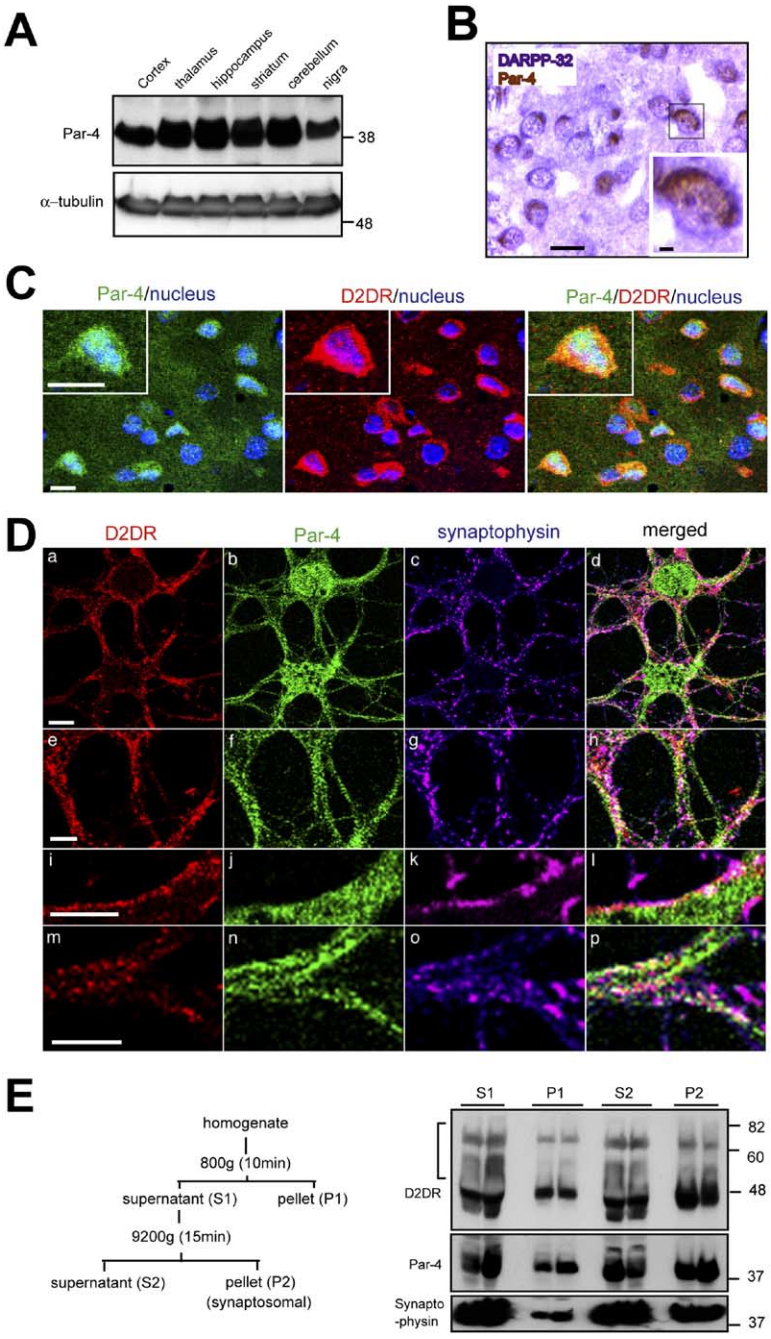

Figure 2. Expression of Par-4 and D2DR

(A) Par-4 expression in various brain regions. Lysates were prepared from indicated mouse brain regions and analyzed by Par-4 Western blot (200 μg protein/lane).

(B) Par-4 expression in DARPP-32-positive neurons in the striatum. Par-4 (DAB/Ni; dark brown) and DARPP-32 (DAB; purple). A higher magnification is shown in the inset. Scale bars, 10 μm in the whole section and 1 μm in the inset.

(C) Colocalization of D2DR and Par-4 in the striatum. A double fluorescence immunostaining of D2DR and Par-4 on the coronal section of a wild-type mouse brain. Green, red, and blue colors indicate Par-4, D2DR, and nucleus (DAPI), respectively. Higher magnifications of a representative cell with significant colocalization are shown in the insets. Scale bars, 10 μm.

(D) Colocalization of Par-4, D2DR, and synaptophysin in cultured mouse striatal neurons (DIV11). Magnified views of processes (panels e–h and m–p) and cell periphery (panels i–l) are also shown. Scale bars represent 2.5 μm in panels (a)–(d) and 1 μm in panels (e)–(l).

(E) Cofractionation of D2DR and Par-4 in the synaptosomal fraction. The schematic fractionation procedure is shown on the left, and a Western blot analysis of equivalent volume of the fractions is on the right. Fractionation was performed in duplicate. The bracket indicates the additional higher-molecular-weight D2DR immunoreactivity.

in the Par-4LZ and receptor construct cotransformants, indicating that Par-4 interaction with D2DR is relatively specific (Figure 1E).

We next examined Par-4 expression in the CNS. Western blot analyses revealed that Par-4 is expressed in various brain regions, including the striatum (Figure 2A). We examined whether Par-4 is expressed in the medium spiny neurons in the striatum, in which most of the dopaminergic inputs are processed (Murer et al., 2002). Indeed, Par-4 is detected in the DARPP-32-positive medium spiny neurons in mouse striatal sections (Figure 2B) (Ouimet et al., 1998). Next, we examined whether D2DR and Par-4 coexpressed in the same cells in the striatum. 90.3% ± 2.6% and 82.7% ± 1.7% of striatal neurons expressed detectable levels of D2DR and Par-4, respectively. The level of Par-4 expression appears variable in different cell types (Figure 2C, Figure S3, and data not shown). The Par-4 positive cells were mostly D2DR-positive (~97%), demonstrating that Par-4 indeed is expressed in D2DR-positive neurons in the striatum. Furthermore, D2DR, Par-4, and synaptophysin colocalize in cultured striatal neurons (Figure 2D). The colocalization is detected primarily in the periphery of the cell soma (Figures 2Da–2Dd and 2Di–2Dl and Figure S4A) and neuronal processes (Figures 2Da–2Dh and 2Dm–2Dp, and Figures S4A and S4B),

where the main pool of functional D2DR is localized (Hersch et al., 1995). Consistently, Par-4 and D2DR cofractionated in the synaptosomal fraction (Figure 2E). Taken together, these results strongly suggest a physiological role for Par-4 in D2DR-mediated dopamine signaling in the striatum, which is likely conferred by its direct interaction with D2i3.

Calmodulin Competes with Par-4 in Binding to D2i3 in a Ca^{2+}-Dependent Manner

The binding domain of D2DR to Par-4 was localized to the first 30 amino acid residues of D2i3 as indicated by in vitro binding assays (Figures 3A–3C). Intriguingly, the binding region (amino acid residues 212–241) harbors the site known to interact with calmodulin (Bofill-Cardona et al., 2000). Indeed, calmodulin binds to D2i3 in a Ca^{2+}-dependent manner (Figure 3D), whereas Par-4LZ binding is constitutive regardless of the presence of Ca^{2+} (Figure 3E). To determine whether Par-4 and calmodulin compete for binding to D2i3, we examined the association of Par-4LZ protein with D2i3 in the presence of increasing levels of calmodulin. An increased binding of calmodulin in the presence of Ca^{2+} interfered with the interaction of Par-4LZ with D2i3 (Figure 3F), indicating that calmodulin can displace Par-4 from D2i3 in a Ca^{2+}-dependent manner. Consistent with the in vitro binding experiments, the coimmunoprecipitation of Par-4 with D2DR-EGFP was significantly reduced in the presence of either ionomycin, a Ca^{2+} ionophore, or thapsigargin, an intracellular Ca^{2+} mobilizer (Lytton et al., 1991) in the stable D2DR-EGFP cell line, indicating that the Par-4/D2DR association can be downregulated by increased Ca^{2+} in the cellular context (Figure 3G).

Par-4 Loss of Function Downregulates D2DR Efficacy to Reduce Inhibitory Tone on Dopamine-Mediated cAMP Signaling

It has been reported previously that calmodulin binding to D2i3 negatively regulates D2DR by interfering with the coupling of the Gi-protein in a noncompetitive manner (Bofill-Cardona et al., 2000). Thus, an equilibrium shift from the Par-4/D2DR interaction to the calmodulin/D2DR interaction by augmented Ca^{2+} concentrations most likely results in a downregulation of D2DR efficacy, thereby relieving the inhibitory tone on dopamine-mediated downstream signaling. To assess the impact of Par-4 loss of function on D2DR efficacy, we sought to silence Par-4 expression, using RNA interference (RNAi) against Par-4 in a DNA-based vector (Sui et al., 2002). The Par-4 siRNA effectively knocked down the expression of endogenous Par-4 protein in the HEK293 cells (Figure 4A) and in cultured rat striatal neurons (Figure 4B). We next analyzed the direct effect of Par-4 loss-of-function on D2DR efficacy by measuring D2DR-mediated inhibition of forskolin-activated adenylyl cyclase activity (Sokoloff et al., 1992) in a stable D2DR-EGFP cell line. While D2DR activation by quinpirole, a D2-like dopamine receptor agonist, resulted in a significant decrease in forskolin-activated cAMP accumulation in mock-transfected cells, the downregulation of adenylate cyclase was not detectable in Par-4 siRNA-transfected cells (Figure 4C). Moreover, Par-4 siRNA produced an enhanced dopamine-mediated cAMP accumulation in cultured rat striatal neurons (Figure 4D). Taken together, these observations indicate that Par-4 loss-of-function negatively affects D2DR efficacy, thereby relieving the inhibitory tone on dopamine-mediated cAMP signaling.

Disruption of the Interaction between Par-4 and D2DR Results in Upregulation of Dopamine-Mediated cAMP Signaling in *Par-4ΔLZ* Striatal Neurons

To further test the physiological relevance of the interaction between Par-4 and D2DR in vivo, we employed a deletion mutant mouse, *Par-4ΔLZ*, that lacks the expression of the C-terminal leucine zipper region of Par-4 that is responsible for interaction with D2DR (Figures 1A, 1B, and 5A) (unpublished data). The knockout of exons 4 and 5 in the Par-4 locus by homologous recombination resulted in expression of the truncated Par-4ΔLZ protein instead of full-length Par-4 in the mutant brain extract (Figure 5B).

To examine the importance of the Par-4/D2DR interaction in dopamine-cAMP signaling in vivo, we analyzed the dopamine-mediated cAMP accumulation in cultured primary striatal neurons derived from wild-type and *Par-4ΔLZ* embryos. No overt morphological differences between cultured striatal neurons from wild-type and *Par-4ΔLZ* embryos were observed (data not shown). Remarkably, mutant neurons exhibited a significantly altered response profile of cAMP levels upon treatment with increasing concentrations of dopamine in comparison with wild-type neurons (Figure 5C). Specifically, 1–10 μM of dopamine markedly elevated cAMP levels in mutant neurons, indicating a reduced inhibitory tone on dopamine-mediated cAMP signaling. The fact that this dopamine concentration is within the physiological range of phasic dopamine in the striatum (Jones et al., 1998), as well as the affinity (K*d*) of dopamine to mammalian D2DR (Bunzow et al., 1988), is noteworthy.

To further delineate the altered cAMP response to dopamine treatment in *Par-4ΔLZ* neurons, we employed D1 and D2 antagonists in the assay. When the SCH23390, a D1DR-specific antagonist, was cotreated with dopamine, the enhancement of cAMP response in *Par-4ΔLZ* neurons was abolished (Figure 5D), indicating that activation of dopamine D1 receptors (D1DR) underlies the cAMP response at 1–10 μM of dopamine. When dopamine and sulpiride, a D2-specific antagonist, were cotreated in the wild-type neurons, the cAMP response was enhanced at 1–10 μM dopamine, which is reminiscent of the increase observed in *Par-4ΔLZ* neurons (Figure 5E, left panel). This result indicates that D2DR activity plays a role in forming an inhibitory tone on the cAMP system in this concentration range. Notably, the D2-specific antagonist revealed no such effect on *Par-4ΔLZ* neurons (Figure 5E, right panel), supporting the idea that D2DR function is impaired in these neurons. Based on these results, it is likely that the decreased inhibitory tone caused by impaired D2DR efficacy in *Par-4ΔLZ* neurons contributes to the concentration-specific upregualtion of the cAMP response.

Dopamine-Dependent CREB Activity Is Upregulated in the Striatal Neurons from *Par-4ΔLZ* Mice

cAMP-responsive element binding protein (CREB) is a downstream transcription factor whose activity is regu-

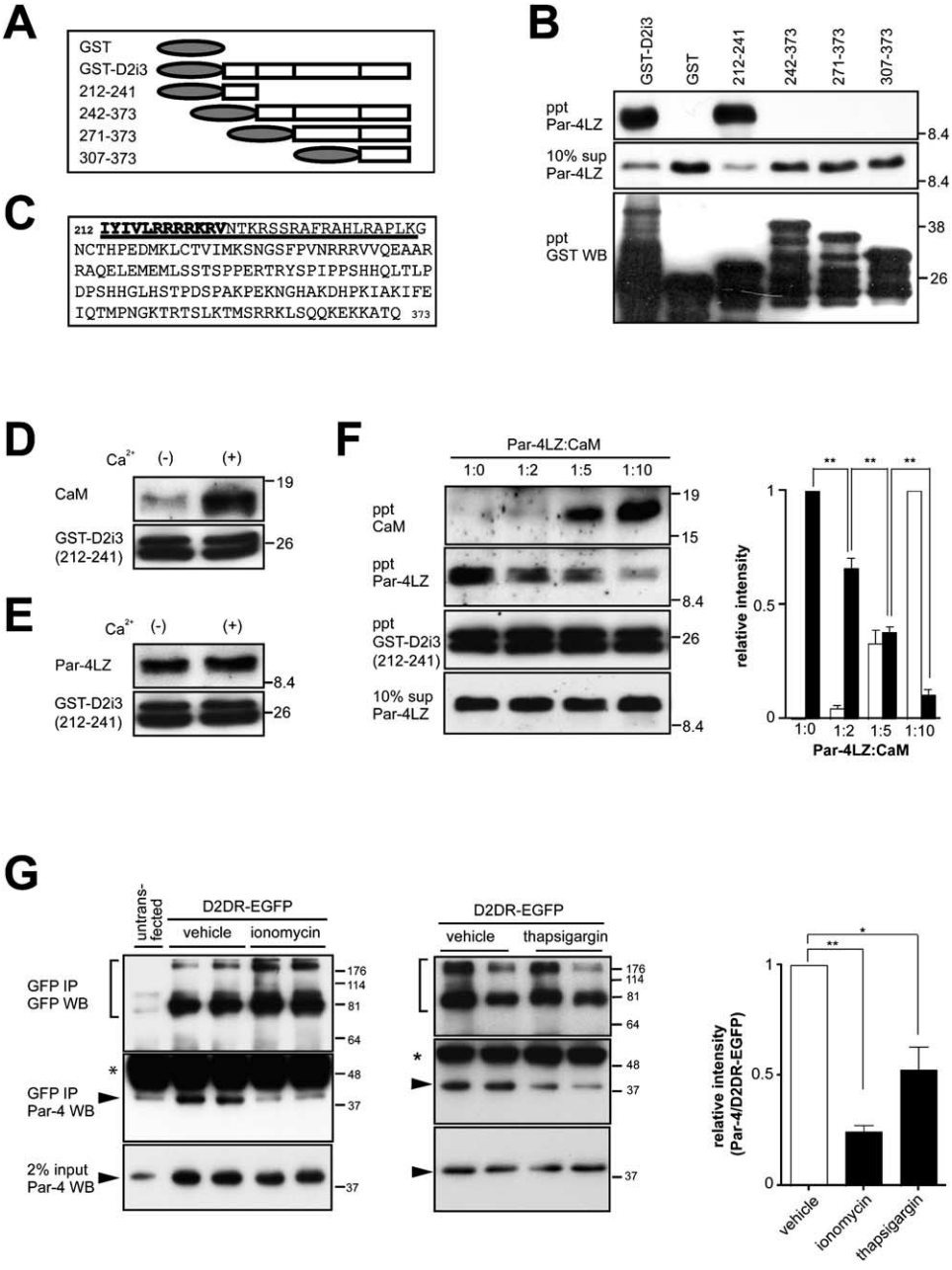

Figure 3. Binding of Par-4 and Calmodulin to a Common Region in the D2i3

(A) Mapping of the Par-4 binding region in D2i3. A series of GST fusion proteins containing D2i3 portions, as indicated, were generated, purified, and used for in vitro binding assays with purified Par-4LZ protein shown in (B).

(B) In vitro binding assays of GST fusion protein shown in (A) with Par-4LZ protein.

(C) Overlap between the Par-4 and calmodulin binding motif in D2i3. The primary sequence of the human D2i3 is shown. Underlined is the region binding to Par-4LZ protein. Bold letters indicate the calmodulin binding motif.

(D) Ca^{2+}-dependent binding of calmodulin to D2i3. CaM, calmodulin.

(E) Constitutive binding of Par-4LZ protein to D2i3.

(F) Competitive binding of Par-4LZ protein and calmodulin. Purified Par-4LZ protein and increasing concentrations of bovine calmodulin were incubated with GST-D2i3$^{212–241}$ protein (50 nmol) in the presence of Ca^{2+} (200 μM) in molar ratios, as indicated, and analyzed by Western blotting. Immunoreactivities for calmodulin (open bars) and Par-4LZ proteins (closed bars) in the GST pulldowns were quantified from scanned images using ImageMaster 2D Elite Software (Amersham Pharmacia). Error bars indicate ±SEM. ** indicates statistical significance as determined by the Student's two-tailed t test; $p \leq 0.01$ (n = 3).

(G) Ca^{2+}-dependent reduction of Par-4/D2DR interaction in HEK293 cells. The stable D2DR-EGFP-expressing HEK293 cell line was treated with ionomycin (2 μM) or thapsigargin (1.5 μM) for 1 hr at room temperature, and the anti-GFP antibody immunoprecipitates were analyzed by Western blotting. Brackets, D2DR-EGFP; closed arrows, Par-4; asterisks, IgG. Immunoreactivities for D2DR-EGFP and endogenous Par-4 were quantified from scanned images using ImageMaster 2D Elite Software (Amersham Pharmacia). Two-tailed t tests: **, $p \leq 0.01$; *, $p \leq 0.05$. n = 4 for ionomycin treatment and n = 2 for thapsigargin treatment.

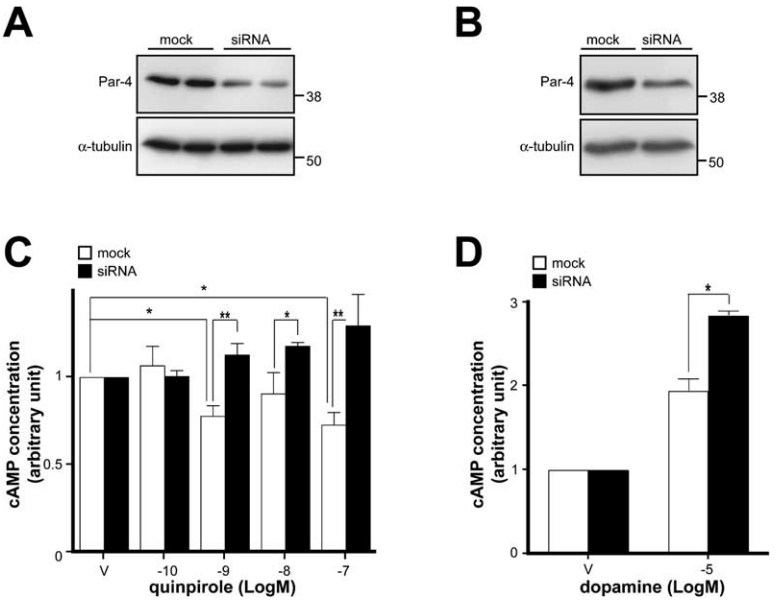

Figure 4. Reduced D2DR Efficacy by Par-4 Loss of Function

(A) Knockdown of the endogenous Par-4 protein by siRNA in HEK293 cells. Lysates from mock (mock)- and Par-4 RNAi-transfected cells (siRNA) were analyzed by Western blotting 48 hr after transfection. Mock, an siRNA construct ineffective on Par-4 expression.

(B) Knockdown of the Par-4 protein by siRNA in the rat striatal neurons. The lysates from rat striatal neurons 3 days after siRNA nucleofection were analyzed by Western blotting.

(C) Forskolin-stimulated cAMP accumulation with increasing concentrations of quinpirole was measured by cAMP enzyme immunoassay in the mock-transfected (open bars) and Par-4 siRNA-transfected cells (closed bars). Statistical significance at each concentration as determined by the Student's two-tailed t test is indicated by asterisks. *, $p \leq .05$; **, $p \leq 0.01$, (n = 3). The overall difference between mock- and Par-4 RNAi-treated samples was statistically significant ($p \leq 0.0005$, two-way ANOVA). Error bars indicate ±SEM. V, vehicle.

(D) The rat striatal neurons were mock-nucleofected (open bars) or nucleofected by Par-4 siRNA (closed bars) before plating and DIV9 neurons treated with vehicle (V) or dopamine for 30 min at room temperature were subjected to the cAMP enzyme immunoassay. Statistical significance was determined by the Student's two-tailed t test; *, $p \leq 0.05$ (n = 2). Error bars indicate ±SEM.

lated by the cAMP-PKA signaling pathway. To examine whether the altered dopamine-mediated cAMP signaling in *Par-4ΔLZ* neurons has further impact on downstream events, we analyzed the phosphorylation status of CREB at serine 133 (S133), a site that is phosphorylated by the cAMP-dependent protein kinase (PKA) in response to dopamine (Figure 5F) (Gonzalez et al., 1989). In wild-type neurons, CREB S133 phosphorylation was significantly decreased upon dopamine treatment in a dose-dependent manner. Interestingly, the dopamine-induced downregulation of CREB S133 phosphorylation was not observed in *Par-4ΔLZ* neurons. When compared to that in wild-type neurons, CREB S133 phosphorylation is markedly upregulated in *Par-4ΔLZ* neurons, which is consistent with the observed upregulation of dopamine-mediated cAMP accumulation in *Par4-ΔLZ* neurons. This result suggests that the downstream events of dopamine-mediated cAMP signaling are affected in the absence of Par-4/D2DR interaction.

Par-4ΔLZ Mice Show Increased Depression-like Behaviors

Dysfunction of the mesolimbic dopamine system is one of the leading candidates for the etiology of certain symptoms characteristic of depression, such as anhedonia and amotivation (American Psychiatric Association, 2000). As such, we tested whether abnormalities in dopamine-mediated signaling in *Par-4ΔLZ* mice have physiological consequences related to depression-like behaviors by employing the Porsolt's forced swim test (FST), a well-established behavioral paradigm to detect depression-like behavior in rodents (Porsolt et al., 1977). Enhanced immobility with no attempt to escape in this test reflects a "depressive mood," as antidepressants were shown to influence this behavior. Remarkably, *Par-4ΔLZ* mice display elevated immobility scores compared to wild-type, hence an increased depression-like behavior (Figure 6A; Supplemental Movies S1 and S2). To verify this result, we performed the tail suspension test (TST), in which a rapid adoption of an immobile posture is shown to reflect a "depressive mood" in rodents (Steru et al., 1985). *Par-4ΔLZ* mice showed significantly elevated immobility scores on the TST compared with those of wild-type mice (Figure 6B; Movies S3 and S4), confirming increased depression-like behaviors in *Par-4ΔLZ* mice. We next tested *Par-4ΔLZ* mice in the novelty-suppressed feeding (NSF) paradigm, which has been used effectively to assess the efficacy of antidepressants by eliciting competing motivations such as the drive to eat and the fear of venturing into the open field (Santarelli et al., 2003). In this test, *Par-4ΔLZ* mice exhibited a significantly increased latency to contact food, indicative of reduced motivation in an aversive environment, a feature of clinical depression (Figure 6C, Movies S5 and S6). In addition, we analyzed behaviors of *Par-4ΔLZ* mice in the open field to determine whether the mutant mouse has abnormalities in exploratory activity, since reduced activity in the open field has been correlated with depression-like behaviors in rodents (El Yacoubi et al., 2003). Indeed, the total exploratory activity of *Par-4ΔLZ* mice in an open field, measured by total distance traveled in the arena, was decreased (Figure 6D and Movies S7 and S8), supporting the depression-like behaviors in *Par-4ΔLZ* mice.

To examine whether the enhanced depression-like behaviors in *Par-4ΔLZ* mice are compromised by a potential anxiety-like behavior, we analyzed the ambulatory pattern of the mice in the open field test, in which

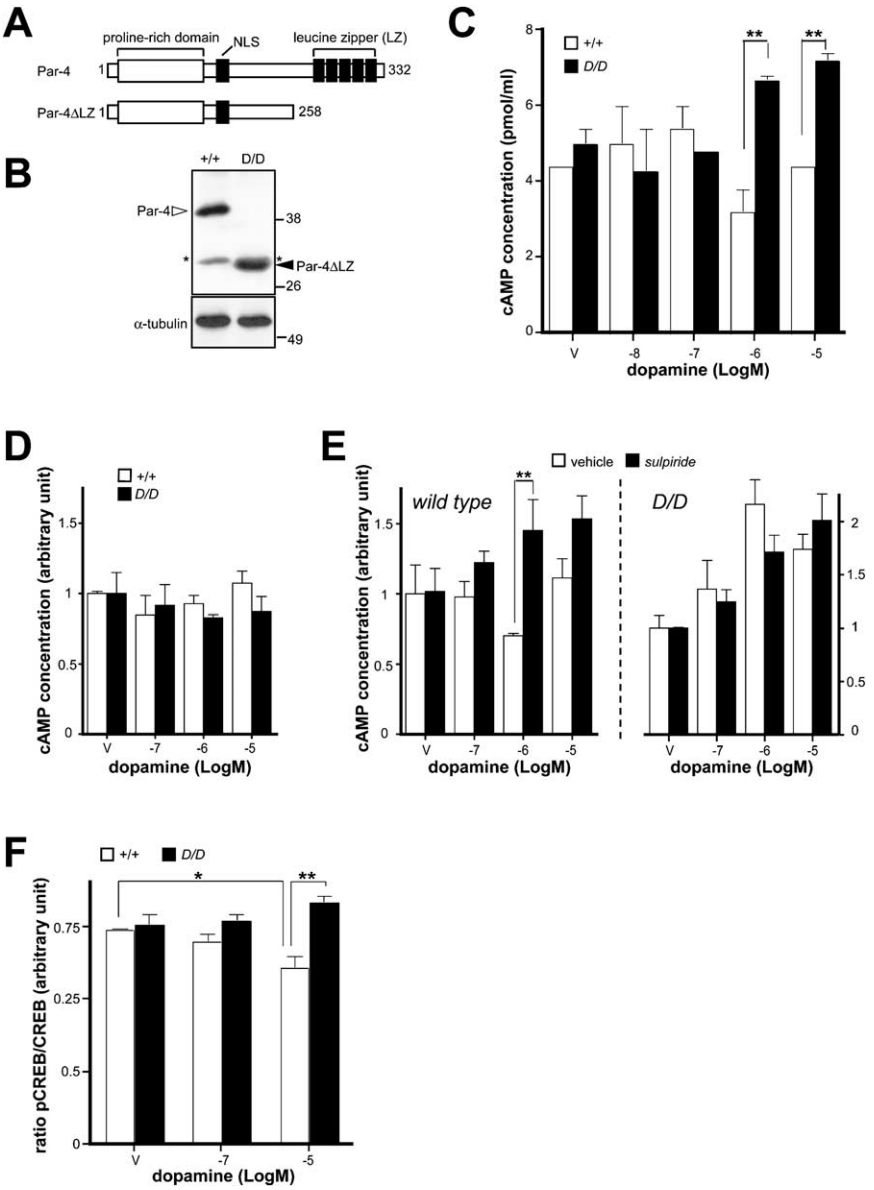

Figure 5. Altered Dopamine-Mediated cAMP Signaling in *Par-4ΔLZ* Mice

(A) A schematic diagram of mouse Par-4 and Par-4ΔLZ proteins.

(B) Expression of truncated Par-4 protein in the *Par-4ΔLZ* mouse. Par-4 protein expression levels in total brain lysates from wild-type and mutant mice were analyzed with Western blotting. Open arrowhead, Par-4; closed arrowhead, Par-4ΔLZ proteins; asterisks, a nonspecific band recognized by anti-Par-4 antibody in both wild-type and *Par-4ΔLZ* brain lysates.

(C) Altered dopamine-stimulated cAMP response profile in *Par-4ΔLZ* neurons. Cultured DIV11 striatal neurons from wild-type (open bars) and *Par-4ΔLZ* mice (closed bars) were treated with increasing concentrations of dopamine, as indicated, and cAMP levels from the cell lysates were measured using cAMP enzyme-immunoassays (n = 4).

(D) Abolished dopamine-mediated cAMP response upon D1-like dopamine receptor antagonist treatment in striatal neurons. Cultured DIV12 striatal neurons from wild-type (open bars) and *Par-4ΔLZ* mice (closed bars) were cotreated with SCH23390 (1 μM) and increasing concentrations of dopamine as indicated, and cAMP levels from the cell lysates were measured (n = 2).

(E) Differential dopamine-stimulated cAMP responses upon D2-like dopamine receptor antagonist treatment. Cultured DIV12 striatal neurons from wild-type (left panel) and *Par-4ΔLZ* embryos (right panel) were treated with increasing concentrations of dopamine in the absence (open bars) or presence of sulpiride (1 μM; closed bars) as indicated, and cAMP levels from the cell lysates were measured (n = 3).

(F) Enhanced dopamine-induced phosphorylation of CREB at serine 133 in *Par-4ΔLZ* neurons. ELISAs for S133 phospho-CREB (pCREB) and total CREB were carried out in the cultured striatal neurons from wild-type (open bars) and *Par-4ΔLZ* mice (closed bars) The DIV11 neurons were treated with increasing concentrations of dopamine as indicated. The ratios of pCREB/CREB were subjected to analyses (n = 3).

Error bars indicate ±SEM. *$p \leq 0.05$, **$p \leq 0.01$; one-way ANOVA. V, vehicle.

the level of center activity has been known to inversely reflect anxiety level (El Yacoubi et al., 2003). The ambulatory pattern and center activities of wild-type and *Par-4ΔLZ* mice were not significantly different, suggesting that anxiety level is not altered in *Par-4ΔLZ* mice (Figure 6E). To further verify this interpretation, we per-

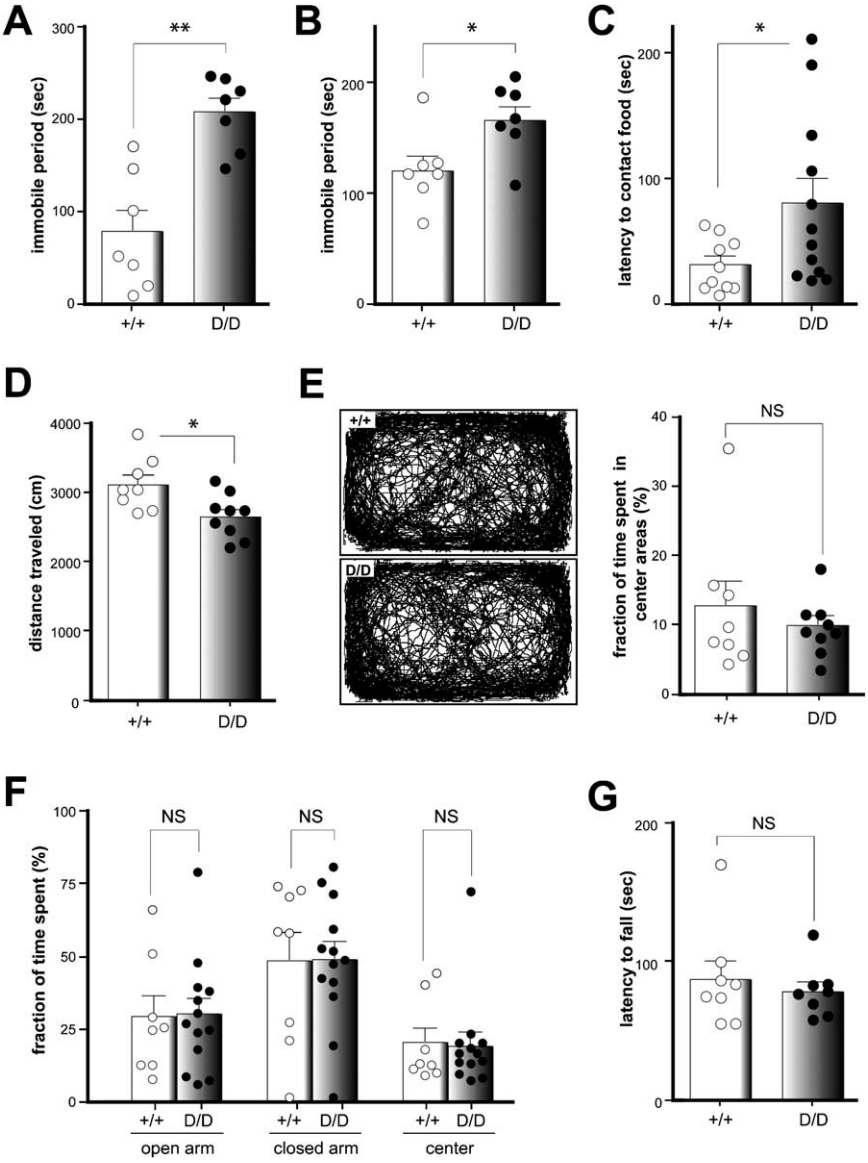

Figure 6. Depression-like Behaviors of *Par-4ΔLZ* Mice

(A) Porsolt's forced swim test (FST). Cumulative immobile period (passive floating without hindleg movements) was measured for a 6 min test session (n = 7/genotype).

(B) Tail suspension test (TST). Cumulative immobile period (no movement of four limbs) was measured for a 6 min test session. (n = 7/genotype).

(C) Novelty-suppressed feeding (NSF). Latency to contact food was analyzed (n = 10 for wild-type and n = 12 for *Par-4ΔLZ* mice).

(D) Exploratory activity in the open field test. Total distance of the mouse traveled in the arena was measured for a 5 min test session (n = 8 for wild-type and n = 9 for *Par-4ΔLZ* mice).

(E) Ambulatory pattern analyses in the open field. Traces of the movements of individual mice in the arena were superimposed (left panel, n = 8/genotype). The arena was subdivided into 16 (4 × 4) rectangular areas, and the time spent in the four center subdivisions was quantified (n = 8 for wild-type and n = 9 for *Par-4ΔLZ* mice).

(F) Elevated plus maze test. Movements of the mice were monitored in the maze and time spent in each area was quantified in a 5 min test session. The fraction of time spent in each area over the total test period was analyzed (n = 8 for wild-type and n = 13 for *Par–4ΔLZ* mice).

(G) Normal motor coordination of *Par-4ΔLZ* mice. Latency to the first fall was analyzed (n = 7/genotype).

Mean values (bars) and individual data points (circles) are plotted. Error bars indicate ±SEM; *p $\leq$ 0.05, ** p $\leq$ 0.01; one-way ANOVA. NS, not significant; +/+, wild-type mice (open bars); D/D, deletion mutants (shaded bars).

formed the elevated plus maze test, a test of anxiety-like behavior (Lister, 1987). In this test, the fraction of time spent in the open and closed arms of the maze was not significantly different between *Par-4ΔLZ* and wild-type mice (Figure 6F; Movie S9), further supporting a normal anxiety level in *Par-4ΔLZ* mice. In addition, no overt anatomical abnormalities of the adult *Par-4ΔLZ* mouse brain were detected (Figure S6), and the performance of *Par-4ΔLZ* mice in a rotarod test was not significantly different from that of wild-type mice (Figure

6G and Movie S10), indicating that the enhanced depression-like behavior of *Par-4ΔLZ* mice is not likely due to defects in brain development and/or motor coordination. Collectively, these results show that a disrupted modulation of dopamine signaling caused by loss of Par-4/D2DR interaction in *Par-4ΔLZ* mice is associated with depression-like behaviors.

Discussion

In the present study, we have reported a function of Par-4 as a modulatory component in dopamine signaling, demonstrating that Par-4/D2DR complex formation is necessary to maintain an inhibitory tone on dopamine-mediated cAMP signaling generated by D2DR in the low Ca^{2+} condition (Figure 7A). A shift in equilibrium toward the calmodulin/D2DR complex can occur when Ca^{2+} influx activates calmodulin, thereby relieving the D2DR-mediated inhibitory tone on cAMP signaling (Figure 7B). Disruption of Par-4/D2DR interaction in *Par-4ΔLZ* mice may facilitate calmodulin/D2DR complex formation upon Ca^{2+} influx, hence an upregulation of dopamine-cAMP-CREB signaling, which may contribute to the increased intensity of depression-like behaviors in the multiple behavioral paradigms tested (Figure 7C). Thus, identification of Par-4/D2DR interaction potentially reveals a mechanism for crosstalk between Ca^{2+} signaling and dopamine-mediated cAMP signaling.

The physiological relevance of the interaction between Par-4 and D2DR and its modulation of cAMP signaling is signified by depression-like behaviors in *Par-4ΔLZ* mice. This observation is of particular interest due to ample evidence suggesting that impairment of dopamine signaling is involved in the manifestation of depression (Manji et al., 2001; Willner, 1995). For example, anhedonia and amotivation, symptoms prominent in depressive patients, are mainly governed by dopamine neurotransmission in reward and motivation circuits (Nader et al., 1997). Moreover, levels of dopamine metabolites in cerebrospinal fluid are reduced in depressive subjects (Bowden et al., 1997). Conversely, a depressive syndrome is frequently encountered in subjects affected by Parkinson's disease, a nigrostriatal hypodopaminergic disorder (Burn, 2002). Notably, D2DR antagonists can induce "pharmacogenic depression" in schizophrenic patients (Willner, 1995), and chronic treatment with antidepressants produces behavioral sensitization to D2DR agonists (Maj et al., 1996). These observations unequivocally suggest that perturbed D2DR-mediated signaling may underlie the manifestation of depressive symptoms and that effects of antidepressants also involve an adaptation of D2DR signaling pathways. Nonetheless, the underlying molecular mechanisms have not been elucidated. In the present study, we have reported perturbed dopamine signaling in *Par-4ΔLZ* mice that is caused by disrupted Par-4/D2DR interaction. Since *Par-4ΔLZ* mice exhibit depression-like behaviors, it is likely that the perturbed dopamine signaling in *Par-4ΔLZ* mice may mimic certain aspects of pathological states of depression at molecular levels, such as an altered CREB activity.

Indeed, roles for cAMP-CREB signaling in the pathophysiology of depression and in the action of antidepressants have been suggested by numerous studies. However, the impact of the changes in cAMP-CREB signaling on the manifestation of depression and the outcome of chronic antidepressant treatment is complex. In some studies, the upregulation of cAMP-CREB is causally correlated with chronic antidepressant effects (Chen et al., 2001; Dowlatshahi et al., 1998). On the other hand, there is also evidence that blockade of cAMP-CREB signaling underlies antidepressant-like effects. For example, repeated antidepressant administration decreases levels of CREB phosphorylation in the frontal cortex (Manier et al., 2002). Furthermore, inhibition of CREB activity in the nucleus accumbens produces an antidepressant-like effect in animal models of depression, whereas overexpression of CREB in

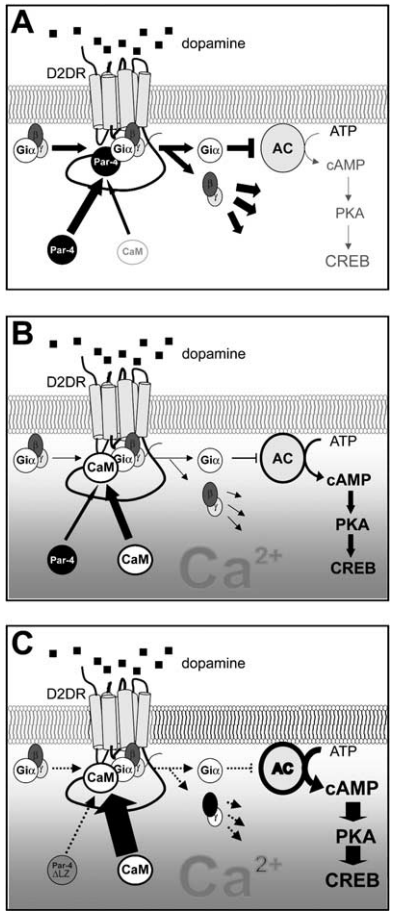

Figure 7. A Model for the Involvement of Par-4 in the Ca^{2+}-Dependent Regulation of D2DR Signaling

Complex formation between Par-4 and D2DR is necessary to maintain the inhibitory tone on cAMP signaling generated by D2DR.
(A) The Ca^2 influx activates calmodulin, shifting the equilibrium toward a calmodulin/D2DR complex. As a result, D2DR efficacy is reduced, thereby relieving D2DR-mediated inhibitory tone on cAMP signaling. (B) Disruption of Par-4/D2DR interaction in *Par-4ΔLZ* mice facilitates calmodulin/D2DR complex formation upon Ca^{2+} influx, hence an upregulation of dopamine-cAMP signaling including the activation of downstream CREB (C). CaM, calmodulin; AC, adenylyl cyclase; PKA, cAMP-dependent protein kinase.

this region elicits opposite effects (Newton et al., 2002; Pliakas et al., 2001). Collectively, it appears that the effect of CREB activity on depression-like behaviors is brain region-specific, mediating differential responses to antidepressants in the nucleus accumbens and other brain regions. In the present study, we have demonstrated an upregulation of dopamine-dependent cAMP-CREB signaling in the striatal neurons from *Par-4ΔLZ* mice in association with depression-like behaviors. This observation is in agreement with reports that an increase in CREB activity in the D2DR-rich nucleus accumbens, a major target of mesolimbic dopaminergic tracts in the striatum, is connected to behavioral responses to emotional stimuli and depressive symptoms (Barrot et al., 2002; Nestler et al., 2002). Thus, the enhanced dopamine-dependent CREB activity and associated changes in the gene expression profile in the reward circuits are likely to contribute to depression-like behaviors in *Par-4ΔLZ* mice.

It is well established that D2DR function is required for normal motor coordination (Viggiano et al., 2003). Interestingly, *Par-4ΔLZ* mice do not exhibit overt defects in motor skills (Figure 6G and Movies S1–S10). We speculate that, by disrupting the direct interaction between D2DR and Par-4, only Par-4-mediated modulatory events in D2DR signaling are impaired in vivo, which may be functionally important only in certain circumstances, such as those related to controlling mood.

The data presented here do not rule out the possibility that the behavioral phenotypes of *Par-4ΔLZ* mice are due to direct modifications, by a similar mechanism, of other neurotransmitter systems such as serotonin or norepinephrine. However, such a possibility is less likely for the following reasons. First, calmodulin-mediated downregulation of D2DR efficacy is relatively specific (Bofill-Cardona et al., 2000). Second, our study of the interaction of Par-4 with the long third intracellular loops of the related G protein-coupled receptors tested did not reveal any significant interaction, indicating that Par-4 does not interact with GPCRs in a promiscuous manner. Third, a comparable upregulation of cAMP signaling upon treatment of serotonin and norepinephrine in *Par-4ΔLZ* striatal neurons was not detected (Figure S7). Nevertheless, given the broad expression of Par-4 in the CNS, additional neuronal functions of Par-4 and the potential contribution of other neural circuits have yet to be determined.

Experimental Procedures

In Vitro Binding Assay

pPC97-D2i3 and pPC86-Par-4LZ plasmids were digested with SalI and NotI and cloned into pGEX4T-2 (Amersham-Pharmacia) using the same restriction sites to make GST-D2i3 and GST-Par-4LZ fusion proteins, respectively. GST fusion proteins were expressed in BL21 bacteria and purified following the manufacturer's instructions. For the in vitro binding assay, 500 nmol of GST-Par-4LZ fusion protein in PBS was digested with 0.2 NIH units thrombin (Sigma) for 2 hr at room temperature, the reaction was stopped by adding 10 μM PMSF (Sigma), and the mixture was incubated for an additional 1 hr at 4°C. The GST portion of the digested protein was removed by glutathione Sepharose (Amersham-Pharmacia). The supernatant was equilibrated to final 1× binding buffer (200 mM NaCl, 0.2% Triton X-100, 0.2 mg/ml BSA, and 50 mM Tris [pH, 7.5]). Binding reaction was initiated by adding 500 nmol of GST-D2i3 (50 nM of GST-D2i3$^{221–241}$ in the competition assay) to Par-4LZ protein in the 1× binding buffer and incubated for 2–3 hr at 4°C. GST-D2i3 was precipitated using 100 μl of 10% glutathione Sepharose in 1× binding buffer. The precipitate was washed three times with 1× binding buffer and resuspended in 2× SDS sample loading buffer.

Antibodies

Anti-Par-4 anti-rabbit polyclonal (R334) (Cheema et al., 2003; Duan et al., 1999a), anti-Par-4 anti-mouse monoclonal (A10) (Bieberich et al., 2003), anti-D2DR anti-goat polyclonal (N19) (Scott et al., 2002), anti-rabbit polyclonal (H50) (Dunah et al., 2002), anti-GST rabbit polyclonal, and monoclonal antibodies were purchased from Santa Cruz Biotechnology. Anti-rabbit anti-DARPP-32 antibody was from Cell Signaling. Anti-synaptophysin (SVP-38) and anti-α-tubulin monoclonal antibodies were from Sigma. Anti-rabbit anti-GFP antibody and Cy5-conjugated anti-mouse IgG were purchased from Molecular Probes. FITC-conjugated anti-rabbit IgG was purchased from ICN, and Texas red-conjugated anti-goat IgG, from Santa Cruz Biotechnology.

Immunoprecipitation

Mice were euthanized in a CO_2 chamber, and the brains were dissected out and Dounce homogenized in the BF2 buffer (150 mM NaCl, 1% NP-40, 0.5% sodium deoxycholate, 0.1% SDS, and 50 mM Tris [pH, 8.0], 5 mM EDTA, 5 mM EGTA, 5 mM glycerol-2-phosphate, 2 mM sodium pyrophosphate, 5 mM NaF, 2 mM Na_3VO_4, 1 mM DTT, phosphatase inhibitor cocktail 1 (Sigma), EDTA-free protease inhibitor cocktail (Roche), and 10 μM ALLM [Calbiochem]). For coimmunoprecipitation using anti Par-4 antibody, the brain was first homogenized in BF1 (150 mM NaCl, 1% NP-40, 50 mM Tris [pH, 8.0], EDTA-free protease inhibitor cocktail (Roche), and 10 μM ALLM [Calbiochem]), centrifuged for 15 min at 12,000× g, and the pellet was resuspended in BF2 and homogenized. The homogenate was centrifuged (10,000× g) and the supernatant was used for immunoprecipitation. Protein extract was incubated with 1μg of antibody on a rocking plate for 1 hr at 4°C. 100 μl 10% protein-G Sepharose (Amersham-Pharmacia) in the same lysis buffer was added and incubated for an additional 45 min at 4°C with gentle shaking. The precipitate was washed three times with lysis buffer and resuspended in 2× SDS sample loading buffer. For D2DR co-immunoprecipitation, anti-D2DR antibodies were conjugated to Dynabeads (DYNAL) following the manufacturer's instruction and incubated with brain lysates. The proteins were eluted in ethanolamine, lyophilized, and dissolved in 2× SDS sample loading buffer. For coimmunoprecipitation from the stable D2DR-EGFP cell line, cells cultured to ~90% confluency in the 10 cm plate were lysed in a lysis buffer (150 mM NaCl, 1% Triton X-100, 5 mM EDTA, 5 mM EGTA, 50 mM Tris [pH, 8.0], 5 mM glycerol-2-phosphate, 2 mM sodium pyrophosphate, 5 mM NaF, 2 mM Na_3VO_4, 1 mM DTT, phosphatase inhibitor cocktail-I (Sigma), EDTA-free protease inhibitor cocktail (Amersham-Pharmacia), 10 μM ALLM [Calbiochem]) for 30 min with gentle shaking at 4°C. Lysates were Dounce homogenized and centrifuged at 12,000 × g for 15 min. Supernatants were used for immunoprecipitation.

Immunohistochemistry

Mice were anesthetized with avertin and perfused transcardially with PBS, followed by 4% paraformaldehyde/PBS. Comparable 6 mm thick paraffin coronal brain sections were deparaffinized and rehydrated. Antigen retrieval was performed by microwave irradiation. Sections were incubated with primary antibodies overnight at 4°C. Bound antibodies were detected by standard streptavidin-biotin-peroxidase methods (Vector Laboratories, Burlingame, CA). Immunostaining was performed using ant-rabbit anti-D2DR (1:50), anti-mouse anti-Par-4 (1:100), and anti-rabbit anti-DARPP-32 (1:100) antibodies.

Immunocytochemistry

DIV11–14 mouse striatal neurons cultured on coverslips were fixed in cold 4% paraformaldehyde/PBS for 1 hr. Coverslips were incubated for 2 hr in the blocking solution (2% goat serum and 1% triton X-100 in PBS), and primary antibodies were incubated for

6–12 hr and secondary antibodies, for 2 hr at room temperature in the blocking solution. Anti-rabbit anti-Par-4 polyclonal antibody was used at a dilution of 1:200, anti-D2DR anti-goat polyclonal antibody, at 1:200, and anti-synaptophysin anti-mouse monoclonal antibody, at 1:300.

cAMP Enzyme-Immunoassay

DIV 11–14 neurons cultured in 24-well plates were replaced with neurobasal media supplemented with 10 mM HEPES (pH, 7.4) containing drugs indicated for 50 min at room temperature; cells were lysed in 200 μl of 0.1 M HCl solution for 15 min with gentle shaking and spun in the microcentrifuge tubes. cAMP concentration of the supernatant was measured using the cAMP-Enzyme Immunoassay Kit (Assay Designs) following the manufacturer's instructions. Concentrations of cAMP were normalized using protein concentrations measured by Biorad Protein Assay System (Bio-Rad).

Forskolin-Activated Adenylate Cyclase Activity Assay

D2DR-mediated inhibition of forskolin-stimulated cAMP production was analyzed in a stable HEK293 cell line expressing D2DR-EGFP. Cells cultured in 24-well dishes were preincubated with rolipram (10 μM) for 15 min and subsequently treated with forskolin (1 μM) and increasing concentrations of quinpirole, as indicated, for 20 min at room temperature. cAMP concentration of the cell lysates was measured by cAMP-EIA.

Behavioral Tests

Porsolt's forced swim test was performed as previously described (Porsolt et al., 1977). Mice were placed in a Plexiglass chamber (diameter, 18 cm; height, 30 cm) filled with water (8 cm deep, 25°C), and immobility (passive floating without hindleg movements) was scored during the 6 min test session. A tail suspension test was carried out as previously described (Steru et al., 1985). A mouse was suspended by the tail to a rod in a shielded chamber. Two blind observers measured the immobility (no foreleg and hindleg movement) during the 6 min test session, and the mean values were used for analysis. Novelty-suppressed feeding behavior was carried out as previously described (Santarelli et al., 2003). Mice were deprived of food for 48 hr and then exposed to the food in a novel context, a white-lit arena (50 × 35cm^2) and monitored using the TSE Videomot 2 video tracking system (TSE Systems). The latency to contact food was analyzed. In the open field test, the exploratory behaviors of the mice were monitored in the 50 × 35cm^2 white-lit arena for 5 min using the TSE Videomot 2. To analyze center activity, the arena was divided into 16 rectangular areas (4 × 4) and time spent in the central four subdivisions was quantified. Elevated plus maze tests were carried out as previously described (Lister, 1987) using the H10-35-EPM system (Coulbourn Instruments). Mice were placed in the center area of the plus maze, and their movements were monitored using TSE Videomot 2. Time spent in the open arms, in the closed arms, and in the center area was quantified. Rotarod tests were performed as previously described (Ona et al., 1999) using the Economex Rotarod System (Columbus Inc.). Prior to testing, mice were trained in three sessions (15 min each) on the same rotarod over a period of 2 days. Latency to fall was measured at 4 – 40 rpm with 1%/s increments in speed.

Supplemental Data

Supplemental Data include Supplemental Experimental Procedures, seven figures, and ten movies and can be found with this article online at http://www.cell.com/cgi/content/full/122/2/275/DC1/.

Acknowledgments

We thank Dr. Lily Moy, Dohoon Kim, and other Tsai lab members, for insightful discussions and comments on the manuscript; Dr. Jay Hirsh, for critical reading of the manuscript; Dr. Lianna Orlando (MGH), for discussion; Dr. Rani Dhavan (UCSF), for technical advice; and Ying Zhou for excellent technical help. We also thank Michelle Ocana and Mark Chafel (HCNR) and Dr. Roderick Bronson (HMS) for technical assistance. This work was supported by grants from Hoechst Marion Roussel and the Amyotrophic Lateral Sclerosis Association to Y.S. L.-H.T. is an investigator at the Howard Hughes Medical Institute. S.K.P. was a fellow of the Taplin Fund Foundation and currently is a recipient of the NARSAD Young Investigator Award. M.D.N. is a holder of the Human Frontier Long-Term Fellowship and A.F. is a fellow of the Humboldt Foundation.

Received: October 26, 2004
Revised: February 3, 2005
Accepted: May 27, 2005
Published: July 28, 2005

References

American Psychiatric Association (2000). Mood disorders. In Diagnostic and Statistical Manual of Mental Disorders, Fourth Edition Text Revision (DSM-IV-TR). (Washington, DC: American Psychiatric Press), pp. 345–428.

Baldessarini, R.J. (1989). Current status of antidepressants: clinical pharmacology and therapy. J. Clin. Psychiatry *50*, 117–126.

Barrot, M., Olivier, J.D., Perrotti, L.I., DiLeone, R.J., Berton, O., Eisch, A.J., Impey, S., Storm, D.R., Neve, R.L., Yin, J.C., et al. (2002). CREB activity in the nucleus accumbens shell controls gating of behavioral responses to emotional stimuli. Proc. Natl. Acad. Sci. USA *99*, 11435–11440.

Bieberich, E., MacKinnon, S., Silva, J., Noggle, S., and Condie, B.G. (2003). Regulation of cell death in mitotic neural progenitor cells by asymmetric distribution of prostate apoptosis response 4 (PAR-4) and simultaneous elevation of endogenous ceramide. J. Cell Biol. *162*, 469–479.

Blazer, D.G., Kessler, R.C., McGonagle, K.A., and Swartz, M.S. (1994). The prevalence and distribution of major depression in a national community sample: the National Comorbidity Survey. Am. J. Psychiatry *151*, 979–986.

Bofill-Cardona, E., Kudlacek, O., Yang, Q., Ahorn, H., Freissmuth, M., and Nanoff, C. (2000). Binding of calmodulin to the D2-dopamine receptor reduces receptor signaling by arresting the G protein activation switch. J. Biol. Chem. *275*, 32672–32680.

Bowden, C., Cheetham, S.C., Lowther, S., Katona, C.L., Crompton, M.R., and Horton, R.W. (1997). Reduced dopamine turnover in the basal ganglia of depressed suicides. Brain Res. *769*, 135–140.

Bunney, W.E., Jr., and Davis, J.M. (1965). Norepinephrine in depressive reactions. A review. Arch. Gen. Psychiatry *13*, 483–494.

Bunzow, J.R., Van Tol, H.H., Grandy, D.K., Albert, P., Salon, J., Christie, M., Machida, C.A., Neve, K.A., and Civelli, O. (1988). Cloning and expression of a rat D2 dopamine receptor cDNA. Nature *336*, 783–787.

Burn, D.J. (2002). Depression in Parkinson's Disease. Eur. J. Neurol. *9*, 44–54.

Cheema, S.K., Mishra, S.K., Rangnekar, V.M., Tari, A.M., Kumar, R., and Lopez-Berestein, G. (2003). Par-4 transcriptionally regulates Bcl-2 through a WT1-binding site on the bcl-2 promoter. J. Biol. Chem. *278*, 19995–20005.

Chen, A.C., Shirayama, Y., Shin, K.H., Neve, R.L., and Duman, R.S. (2001). Expression of the cAMP response element binding protein (CREB) in hippocampus produces an antidepressant effect. Biol. Psychiatry *49*, 753–762.

Coppen, A. (1967). The biochemistry of affective disorders. Br. J. Psychiatry *113*, 1237–1264.

De Camilli, P., Macconi, D., and Spada, A. (1979). Dopamine inhibits adenylate cyclase in human prolactin-secreting pituitary adenomas. Nature *278*, 252–254.

Delay, J., Laine, B., and Buisson, J.F. (1952). Ann. Med. Psychol. (Paris) *110*, 689–692.

Diaz-Meco, M.T., Municio, M.M., Frutos, S., Sanchez, P., Lozano, J., Sanz, L., and Moscat, J. (1996). The product of par-4, a gene induced during apoptosis, interacts selectively with the atypical isoforms of protein kinase C. Cell *86*, 777–786.

Diaz-Meco, M.T., Lallena, M.J., Monjas, A., Frutos, S., and Moscat,

J. (1999). Inactivation of the inhibitory kappaB protein kinase/nuclear factor kappaB pathway by Par-4 expression potentiates tumor necrosis factor alpha-induced apoptosis. J. Biol. Chem. *274*, 19606–19612.

Dowlatshahi, D., MacQueen, G.M., Wang, J.F., and Young, L.T. (1998). Increased temporal cortex CREB concentrations and antidepressant treatment in major depression. Lancet *352*, 1754–1755.

Duan, W., Rangnekar, V.M., and Mattson, M.P. (1999a). Prostate apoptosis response-4 production in synaptic compartments following apoptotic and excitotoxic insults: evidence for a pivotal role in mitochondrial dysfunction and neuronal degeneration. J. Neurochem. *72*, 2312–2322.

Duan, W., Zhang, Z., Gash, D.M., and Mattson, M.P. (1999b). Participation of prostate apoptosis response-4 in degeneration of dopaminergic neurons in models of Parkinson's disease. Ann. Neurol. *46*, 587–597.

Dunah, A.W., Jeong, H., Griffin, A., Kim, Y.M., Standaert, D.G., Hersch, S.M., Mouradian, M.M., Young, A.B., Tanese, N., and Krainc, D. (2002). Sp1 and TAFII130 transcriptional activity disrupted in early Huntington's disease. Science *296*, 2238–2243.

El Yacoubi, M., Bouali, S., Popa, D., Naudon, L., Leroux-Nicollet, I., Hamon, M., Costentin, J., Adrien, J., and Vaugeois, J.M. (2003). Behavioral, neurochemical, and electrophysiological characterization of a genetic mouse model of depression. Proc. Natl. Acad. Sci. USA *100*, 6227–6232.

Fishburn, C.S., Elazar, Z., and Fuchs, S. (1995). Differential glycosylation and intracellular trafficking for the long and short isoforms of the D2 dopamine receptor. J. Biol. Chem. *270*, 29819–29824.

Fuller, R.W. (1995). Serotonin uptake inhibitors: uses in clinical therapy and in laboratory research. Prog. Drug Res. *45*, 167–204.

Gonzalez, G.A., Yamamoto, K.K., Fischer, W.H., Karr, D., Menzel, P., Biggs, W., 3rd, Vale, W.W., and Montminy, M.R. (1989). A cluster of phosphorylation sites on the cyclic AMP-regulated nuclear factor CREB predicted by its sequence. Nature *337*, 749–752.

Greenberg, P.E., Stiglin, L.E., Finkelstein, S.N., and Berndt, E.R. (1993). The economic burden of depression in 1990. J. Clin. Psychiatry *54*, 405–418.

Guo, Q., Fu, W., Xie, J., Luo, H., Sells, S.F., Geddes, J.W., Bondada, V., Rangnekar, V.M., and Mattson, M.P. (1998). Par-4 is a mediator of neuronal degeneration associated with the pathogenesis of Alzheimer disease. Nat. Med. *4*, 957–962.

Hersch, S.M., Ciliax, B.J., Gutekunst, C.A., Rees, H.D., Heilman, C.J., Yung, K.K., Bolam, J.P., Ince, E., Yi, H., and Levey, A.I. (1995). Electron microscopic analysis of D1 and D2 dopamine receptor proteins in the dorsal striatum and their synaptic relationships with motor corticostriatal afferents. J. Neurosci. *15*, 5222–5237.

Jarvie, K.R., and Niznik, H.B. (1989). Deglycosylation and proteolysis of photolabeled D2 dopamine receptors of the porcine anterior pituitary. J. Biochem. (Tokyo) *106*, 17–22.

Johnstone, R.W., See, R.H., Sells, S.F., Wang, J., Muthukkumar, S., Englert, C., Haber, D.A., Licht, J.D., Sugrue, S.P., Roberts, T., et al. (1996). A novel repressor, par-4, modulates transcription and growth suppression functions of the Wilms' tumor suppressor WT1. Mol. Cell. Biol. *16*, 6945–6956.

Jones, S.R., Gainetdinov, R.R., Wightman, R.M., and Caron, M.G. (1998). Mechanisms of amphetamine action revealed in mice lacking the dopamine transporter. J. Neurosci. *18*, 1979–1986.

Kinney, J.L. (1985). Nomifensine maleate: a new second-generation antidepressant. Clin. Pharm. *4*, 625–636.

Kuhn, R. (1958). The treatment of depressive states with G 22355 (imipramine hydrochloride). Am. J. Psychiatry *115*, 459–464.

Leonard, B.E. (1978). Mianserin, an antidepressant with a unique neuropharmacological profile. Acta Psychiatr. Belg. *78*, 770–780.

Lister, R.G. (1987). The use of a plus-maze to measure anxiety in the mouse. Psychopharmacology (Berl.) *92*, 180–185.

Lytton, J., Westlin, M., and Hanley, M.R. (1991). Thapsigargin inhibits the sarcoplasmic or endoplasmic reticulum Ca-ATPase family of calcium pumps. J. Biol. Chem. *266*, 17067–17071.

Maj, J., Dziedzicka-Wasylewska, M., Rogoz, R., Rogoz, Z., and Skuza, G. (1996). Antidepressant drugs given repeatedly change the binding of the dopamine D2 receptor agonist, [3H]N-0437, to dopamine D2 receptors in the rat brain. Eur. J. Pharmacol. *304*, 49–54.

Manier, D.H., Shelton, R.C., and Sulser, F. (2002). Noradrenergic antidepressants: does chronic treatment increase or decrease nuclear CREB-P? J. Neural Transm. *109*, 91–99.

Manji, H.K., Drevets, W.C., and Charney, D.S. (2001). The cellular neurobiology of depression. Nat. Med. *7*, 541–547.

Missale, C., Nash, S.R., Robinson, S.W., Jaber, M., and Caron, M.G. (1998). Dopamine receptors: from structure to function. Physiol. Rev. *78*, 189–225.

Murer, M.G., Tseng, K.Y., Kasanetz, F., Belluscio, M., and Riquelme, L.A. (2002). Brain oscillations, medium spiny neurons, and dopamine. Cell. Mol. Neurobiol. *22*, 611–632.

Nader, K., Bechara, A., and van der Kooy, D. (1997). Neurobiological constraints on behavioral models of motivation. Annu. Rev. Psychol. *48*, 85–114.

Nestler, E.J. (2001). Molecular neurobiology of addiction. Am. J. Addict. *10*, 201–217.

Nestler, E.J., Barrot, M., DiLeone, R.J., Eisch, A.J., Gold, S.J., and Monteggia, L.M. (2002). Neurobiology of depression. Neuron *34*, 13–25.

Newton, S.S., Thome, J., Wallace, T.L., Shirayama, Y., Schlesinger, L., Sakai, N., Chen, J., Neve, R., Nestler, E.J., and Duman, R.S. (2002). Inhibition of cAMP response element-binding protein or dynorphin in the nucleus accumbens produces an antidepressant-like effect. J. Neurosci. *22*, 10883–10890.

Ona, V.O., Li, M., Vonsattel, J.P., Andrews, L.J., Khan, S.Q., Chung, W.M., Frey, A.S., Menon, A.S., Li, X.J., Stieg, P.E., et al. (1999). Inhibition of caspase-1 slows disease progression in a mouse model of Huntington's disease. Nature *399*, 263–267.

Ouimet, C.C., Langley-Gullion, K.C., and Greengard, P. (1998). Quantitative immunocytochemistry of DARPP-32-expressing neurons in the rat caudatoputamen. Brain Res. *808*, 8–12.

Pedersen, W.A., Luo, H., Kruman, I., Kasarskis, E., and Mattson, M.P. (2000). The prostate apoptosis response-4 protein participates in motor neuron degeneration in amyotrophic lateral sclerosis. FASEB J. *14*, 913–924.

Pliakas, A.M., Carlson, R.R., Neve, R.L., Konradi, C., Nestler, E.J., and Carlezon, W.A., Jr. (2001). Altered responsiveness to cocaine and increased immobility in the forced swim test associated with elevated cAMP response element-binding protein expression in nucleus accumbens. J. Neurosci. *21*, 7397–7403.

Porsolt, R.D., Le Pichon, M., and Jalfre, M. (1977). Depression: a new animal model sensitive to antidepressant treatments. Nature *266*, 730–732.

Santarelli, L., Saxe, M., Gross, C., Surget, A., Battaglia, F., Dulawa, S., Weisstaub, N., Lee, J., Duman, R., Arancio, O., et al. (2003). Requirement of hippocampal neurogenesis for the behavioral effects of antidepressants. Science *301*, 805–809.

Schildkraut, J.J., Gordon, E.K., and Durell, J. (1965). Catecholamine metabolism in affective disorders. I. Normetanephrine and VMA excretion in depressed patients treated with imipramine. J. Psychiatr. Res. *3*, 213–228.

Scott, L., Kruse, M.S., Forssberg, H., Brismar, H., Greengard, P., and Aperia, A. (2002). Selective up-regulation of dopamine D1 receptors in dendritic spines by NMDA receptor activation. Proc. Natl. Acad. Sci. USA *99*, 1661–1664.

Sells, S.F., Wood, D.P., Jr., Joshi-Barve, S.S., Muthukumar, S., Jacob, R.J., Crist, S.A., Humphreys, S., and Rangnekar, V.M. (1994). Commonality of the gene programs induced by effectors of apoptosis in androgen-dependent and -independent prostate cells. Cell Growth Differ. *5*, 457–466.

Sokoloff, P., Andrieux, M., Besancon, R., Pilon, C., Martres, M.P., Giros, B., and Schwartz, J.C. (1992). Pharmacology of human dopamine D3 receptor expressed in a mammalian cell line: comparison with D2 receptor. Eur. J. Pharmacol. *225*, 331–337.

Steru, L., Chermat, R., Thierry, B., and Simon, P. (1985). The tail

suspension test: a new method for screening antidepressants in mice. Psychopharmacology (Berl.) *85*, 367–370.

Sui, G., Soohoo, C., Affar el, B., Gay, F., Shi, Y., and Forrester, W.C. (2002). A DNA vector-based RNAi technology to suppress gene expression in mammalian cells. Proc. Natl. Acad. Sci. USA *99*, 5515–5520.

Viggiano, D., Ruocco, L.A., and Sadile, A.G. (2003). Dopamine phenotype and behaviour in animal models: in relation to attention deficit hyperactivity disorder. Neurosci. Biobehav. Rev. *27*, 623–637.

Willner, P. (1995). Dopaminergic mechanisms in depression and mania. In Psychopharmacology: The Fourth Generation of Progress, F.E. Bloom and D.I. Kupfer, eds. (New York: Raven), pp. 921–932.

Wong, M.L., and Licinio, J. (2001). Research and treatment approaches to depression. Nat. Rev. Neurosci. *2*, 343–351.